

# Evidence for a disordered critical point in a glass-forming liquid

Ludovic Berthier<sup>1</sup> and Robert L. Jack<sup>2</sup>

<sup>1</sup>Laboratoire Charles Coulomb, UMR 5221 CNRS-Université de Montpellier, Montpellier, France

<sup>2</sup>Department of Physics, University of Bath, Bath, BA2 7AY, United Kingdom

(Dated: August 20, 2018)

Using computer simulations of an atomistic glass-forming liquid, we investigate the fluctuations of the overlap between a fluid configuration and a quenched reference system. We find that large fluctuations of the overlap develop as temperature decreases, consistent with the existence of the random critical point that is predicted by effective field theories. We discuss the scaling of fluctuations near the presumed critical point, comparing the observed behaviour with that of the random-field Ising model. We argue that this critical point directly reveals the existence of an interfacial tension between amorphous metastable states, a quantity relevant both for equilibrium relaxation and for nonequilibrium melting of stable glass configurations.

PACS numbers: 05.10.-a, 05.20.Jj, 64.70.Q-

In the search for a theory of the glass transition, an important question is whether the slow dynamics of supercooled liquids can be explained in terms of the temperature evolution of ‘universal’ thermodynamic quantities, independent on the details of the material [1]. Two-body density correlators, which are central to the theory of simple liquids [2], fail for viscous liquids [3]. In the framework of the random first-order transition (RFOT) theory [4], slow dynamics is described in terms of infrequent transitions between amorphous free energy minima, separated by large barriers. Structural relaxation is interpreted as the nucleation of one metastable state into another [5]. This physical picture is supported by mean-field calculations of a free-energy  $V(Q)$ . Here, the overlap  $Q$  measures the similarity between pairs of configurations: it acts as an order parameter for the glass transition [6]. This ‘Landau free energy’ describes the overlap fluctuations and links statics to dynamics. Because they embody high-order density correlations, overlap fluctuations are key candidates to construct a thermodynamic theory of the glass transition and, as such, are currently the focus of a large interest [7–13]. The central challenge, tackled here, is to understand whether the rigorous results obtained in the mean-field limit are relevant for realistic, finite dimensional liquids.

At mean-field level,  $V(Q)$  allows for a compact description of the liquid-glass phase transition occurring at the Kauzmann temperature,  $T_K$ , for which  $Q$  is the relevant order parameter. By introducing additional external fields, such as a coupling  $\epsilon$  to a reference copy of the system, the glass transition at  $(T = T_K, \epsilon = 0)$  transforms in a first-order transition line ending at a critical point at  $(T_c, \epsilon_c > 0)$  [6, 11, 14]. Because  $T_c > T_K$ , this critical point might be more easily accessible than  $T_K$ . This scenario occurs in some disordered spin models but has not been demonstrated in equilibrium calculations on atomistic systems (see [7, 15, 16] for earlier work). Here, we present free-energy calculations that provide direct evidence for such a critical point in a realistic glass-former,

and find a critical behaviour consistent with the universality class of the random field ising model (RFIM), in agreement with theory [12, 13]. Further motivation to analyse this critical point is that its absence would directly establish that a Kauzmann transition does not occur at any  $T_K > 0$ . (The reverse is not true: a finite  $T_c$  does not imply a finite  $T_K$ .) The existence of a first-order transition line at  $T < T_c$  is even more significant for understanding glassy phenomenology because it is associated with phase coexistence between equivalent metastable states. In particular, the corresponding interfacial tension,  $\Upsilon(T)$ , is an important piece of the RFOT theory [5, 17], but even establishing its existence has proven difficult in computational studies [7, 18, 19]. Our approach bypasses these problems and paves the way for direct quantitative determinations of  $\Upsilon$ . As a first step, we analyse cases where stable glass states coexist with liquid states, with a large barrier between them that we attribute to an interfacial free energy. This finding is relevant to the current effort to understand the melting process of ultrastable glasses [21–23].

We consider a well-studied binary mixture of Lennard-Jones particles [24], which exhibits glassy dynamics below  $T \approx 1.0$ . The unit of length is the diameter of the larger particles, the unit of energy is the pair-interaction scale, the Boltzmann constant is unity, and the total number of particles is  $N$ . The position of particle  $i$  is  $\mathbf{r}_i$ , and  $\mathcal{C} = (\mathbf{r}_1, \mathbf{r}_2, \dots, \mathbf{r}_N)$  denotes a configuration of the system. Following [6], we simulate two copies of the system. First, a *reference configuration*  $\mathcal{C}_0$  is drawn at random from the equilibrium state of the model at temperature  $T'$ . Then, we perform Monte-Carlo (MC) simulations on a second configuration  $\mathcal{C}$ , which is biased by a field  $\epsilon$  to lie close to  $\mathcal{C}_0$ . Specifically, our MC method samples configurations  $\mathcal{C}$  according to the Boltzmann weight for the Hamiltonian  $E(\mathcal{C}) - \epsilon Q(\mathcal{C}, \mathcal{C}_0)$ , where  $E$  is the potential energy and  $Q(\mathcal{C}, \mathcal{C}') = \frac{1}{N} \sum_{ij} \Theta(a - |\mathbf{r}_i - \mathbf{r}'_j|)$  is the overlap between configurations  $\mathcal{C}$  and  $\mathcal{C}'$ . Here,  $\Theta(x)$  is the Heaviside function and we take  $a = 0.3$ . Efficiently

sampling this Hamiltonian is challenging, and we adopt the strategy detailed in [9, 10] which combines parallel tempering with umbrella sampling and reweighting techniques. Using this approach we were able to study system sizes  $N = 150, 256$  for temperatures  $T \geq 0.55$ .

The temperatures  $T$  and  $T'$  may be different ( $\mathcal{C}_0$  need not even be thermalized), but the case  $T = T'$  has special importance. For  $\epsilon = 0$ ,  $\mathcal{C}$  and  $\mathcal{C}_0$  are independent. As  $\epsilon$  increases, the configurations become more similar and their mutual overlap grows. Our goal is to investigate the presence of singularities in overlap fluctuations in the  $(\epsilon, T)$  plane. To this end, a central role is played by the ( $\epsilon$ -dependent) distribution of the overlap,  $P(Q)$ . This distribution is obtained by first performing a thermal average over  $\mathcal{C}$ , and then averaging the results over reference configurations  $\mathcal{C}_0$  (we typically use 60 independent configurations for each  $T$  and  $N$ ). This double average is indicated with simple brackets  $\langle \cdot \rangle$ .

We emphasize that the reference configuration  $\mathcal{C}_0$  is fixed (or ‘quenched’) within each simulation, and sampling is restricted to configuration  $\mathcal{C}$ . This approach is relevant for glassy systems, because we expect  $\mathcal{C}_0$  to be representative of equilibrium metastable states at temperature  $T'$ . The configuration  $\mathcal{C}$ , at temperature  $T$ , may then either occupy the same metastable state (when  $Q$  is large) or a different one (when  $Q$  is low). If phase coexistence occurs at  $T' = T$ , then *it takes place between equivalent metastable states*. The ‘annealed’ case in which both configurations fluctuate is qualitatively different because the high- $Q$  configurations are not representative equilibrium states [9, 25–29].

In Fig. 1 we show results for  $T' = T$ . The isotherms  $\langle Q \rangle(\epsilon, T)$  shown in Fig. 1(a) recall the relationship between pressure and density in a liquid-vapor system. On lowering the temperature, they become increasingly flat. This evolution is more pronounced for the larger system. Below the critical point, one would observe, in the thermodynamic limit, horizontal tie-lines associated with phase coexistence. Fig. 1(b) shows the susceptibility  $\chi(\epsilon, T) = N(\langle Q^2 \rangle - \langle Q \rangle^2)$ , which exhibits a pronounced maximum at a field  $\epsilon^*(T)$  that shifts to lower values when  $T$  decreases, suggesting a reduction in the thermodynamic cost of localizing the system near a reference configuration (related to the configurational entropy). Interestingly  $\chi(\epsilon^*, T)$  grows rapidly as  $T$  is lowered, and also increases strongly with system size. This behavior is expected if the system approaches a critical point, but can also be obtained if a correlation length larger than the system size develops. The evolution of  $\epsilon^*(T)$  is shown in Fig. 1(c) in the  $(\epsilon, T)$  phase diagram. In the liquid-vapor analogy, this corresponds to the critical isochore and, for temperatures above the critical point, to a Widom line [30]. The observed linear decrease of  $\epsilon^*$  with  $T$  is consistent with mean-field theories.

Finally, Fig. 1(d) shows the free energy  $V(Q) = (-T/N) \log P(Q)$  measured at various  $T$ , for  $\epsilon = 0$ . It

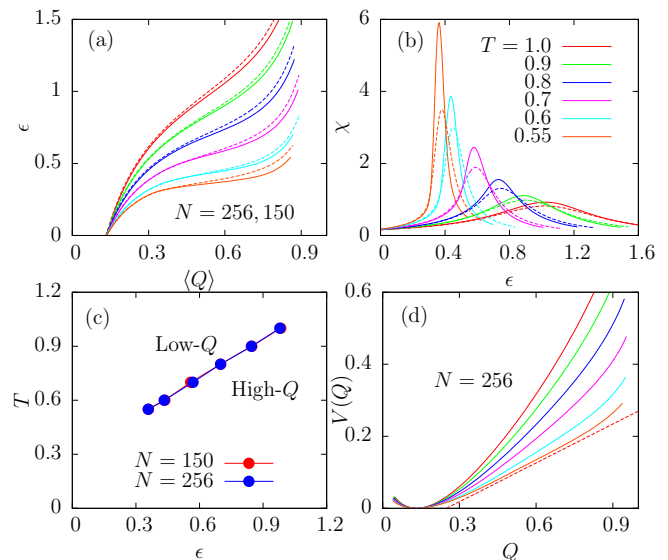


FIG. 1: (a) Dependence of the average overlap  $\langle Q \rangle$  on the field  $\epsilon$  along various isotherms for  $N = 256$  (full) and  $N = 150$  (dashed). The behaviour is reminiscent of isotherms in a liquid-vapor system. (b) Total susceptibility  $\chi(\epsilon, T)$  for the same parameters showing increasing fluctuations as temperature is reduced and system size is increased. (c) Temperature-dependence of the field  $\epsilon^*$  that maximises  $\chi$ , indicating the boundary between low- $Q$  and high- $Q$  regimes. (d) Free energy  $V(Q)$  for the same temperatures as in (a, b) for  $N = 256$ , with a dashed line indicating linear behavior.

has the usual convex form at high  $T$  with a minimum near  $Q \approx 0$ . For lower  $T$  and intermediate values of  $Q$ , its curvature decreases markedly, consistent with the increasing variance of  $Q$ . For  $T < T_c$ , one expects  $V(Q)$  to acquire a region of zero curvature, due to Maxwell’s construction, similar to the behavior shown at the lowest studied temperature  $T = 0.55$ . Whereas the value of  $V(Q)$  in the high-overlap regime provides a direct estimate of the configurational entropy [10], the postulated surface tension  $\Upsilon(T)$  between states cannot be obtained directly from  $V(Q)$ .

To gain further insight, we analyse the overlap distribution,  $P(Q)$ , because it can better reveal critical fluctuations and phase coexistence. We show in Fig. 2(a) the temperature evolution of these distributions evaluated along the  $\epsilon^*(T)$  line. The distribution is narrow and essentially Gaussian at high temperature,  $T \geq 0.7$ . It becomes broader, develops a non-Gaussian flat center, and eventually becomes weakly bimodal for  $T = 0.55$ ,  $N = 256$ . Bimodality is more pronounced for the largest system. To investigate this  $N$ -dependence, we calculated the Binder cumulant ratio  $B = \langle (Q - \langle Q \rangle)^2 \rangle^2 / \langle (Q - \langle Q \rangle)^4 \rangle$ . On a first-order transition line,  $B$  increases with  $N$ , tending to unity as  $N \rightarrow \infty$  whereas above  $T_c$  it decreases with  $N$  towards  $\frac{1}{3}$ . At  $T_c$ ,  $B$  is size-independent with a limiting value intermediate between  $\frac{1}{3}$  and unity. At high temperatures, we find  $B \approx \frac{1}{3}$  as expected, and for

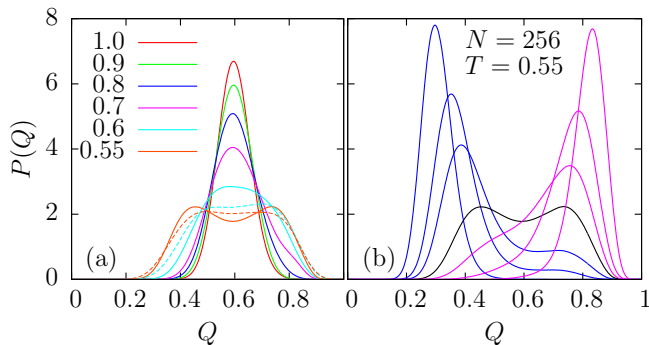


FIG. 2: (a) Overlap distributions  $P(Q)$  measured along the  $\epsilon^*(T)$  line for  $N = 256$  (full lines); dotted lines are for  $N = 150$  and  $T = 0.6$  and  $0.55$ . For the lowest temperature, a bimodal structure appears. (b) Behaviour of  $P(Q)$  for various  $\epsilon$ , increasing from low- $\epsilon$  (blue) to  $\epsilon = \epsilon^*$  (black) and large- $\epsilon$  (purple) for  $N = 256$  and  $T = 0.55$ .

$T = 0.55$  and  $N = (150, 256)$ , we get  $B = (0.48, 0.52)$ , consistent with this temperature being close to  $T_c$ , although our range of system sizes is rather small. For  $T = 0.55$ ,  $N = 256$  we show  $P(Q)$  in Fig. 2(b), which evolves from a unimodal distribution at low- $Q$  when  $\epsilon < \epsilon^*$  to a similarly unimodal distribution at high  $Q$  when  $\epsilon > \epsilon^*$ , with an intermediate bimodal distribution at  $\epsilon^*$ . This evolution is qualitatively consistent with the crossing of a first-order-like transition line in a finite-size system, but systematic finite-size scaling is needed to draw conclusions about the thermodynamic limit.

Random critical points in systems with quenched disorder have distinct properties from standard liquid-vapor transitions [31]. In particular, the system may behave differently for different realizations of the disorder [32], in our case different reference configurations  $\mathcal{C}_0$ . It is thus useful to decompose averages, using  $\langle \cdot \rangle_{\mathcal{C}_0}$  for a thermal average over  $\mathcal{C}$  at fixed  $\mathcal{C}_0$ , and an overbar  $\overline{(\cdot)}$  for a disorder average over  $\mathcal{C}_0$ . We find that the isotherms  $\langle Q \rangle_{\mathcal{C}_0}$  have strong sample-to-sample fluctuations. The overlap grows more or less abruptly with  $\epsilon$  for different samples, so that the critical field  $\epsilon_{\mathcal{C}_0}^*$  is a distributed quantity. In Fig. 3(a) we show that at low temperature,  $T = 0.55$ , the distribution of  $\epsilon_{\mathcal{C}_0}^*$  is so broad that the distributions  $P(Q)$  for most samples at the average value  $\epsilon^* = \overline{\epsilon_{\mathcal{C}_0}^*}$  are dominated by either their small- $Q$  or large- $Q$  peaks. Most of these distributions do become bimodal when the field is adjusted to  $\epsilon_{\mathcal{C}_0}^*$  for each sample separately. These results strongly suggest that the quenched disorder plays a significant role in the overlap fluctuations.

In mapping the supercooled liquid to the RFIM, the configuration  $\mathcal{C}$  corresponds to an Ising model in a random magnetic field, and the specific realisation of the disorder corresponds to  $\mathcal{C}_0$ . In the RFIM, each realisation of the random field slightly favors either positive or negative magnetisation. As a result, each sample typically has only one thermally-populated state [32], in con-

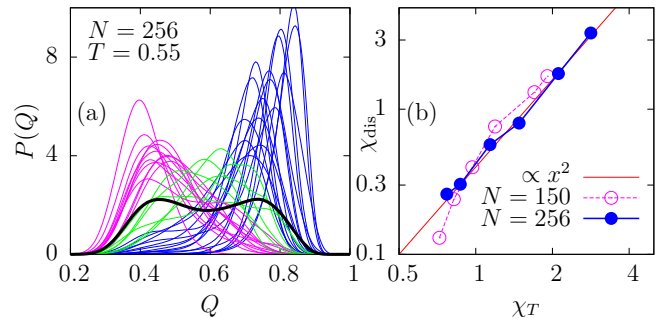


FIG. 3: (a) Sample-to-sample fluctuations of the distributions  $P(Q)$  for  $T = 0.55$ ,  $N = 256$  evaluated at the average  $\epsilon^*$ . Colors indicate whether the samples are predominately in high-, intermediate, or low- $Q$  states. As expected for RFIM behaviour, most distributions are unimodal, averaging to a total bimodal distribution (black). (b) Temperature dependence of the susceptibilities  $\chi_{\text{dis}}$  and  $\chi_T$  measured at  $\epsilon^*$ . The solid line is the RFIM prediction, Eq. (1).

strast to the pure case for which both states are equally likely. In large systems, this disorder effect dominates the critical fluctuations, which changes the universality class from Ising to RFIM.

For quantitative analysis, we decompose fluctuations into thermal,  $\chi_T = N(\overline{\langle Q^2 \rangle_{\mathcal{C}_0}} - \overline{\langle Q \rangle_{\mathcal{C}_0}^2})$ , and disorder parts,  $\chi_{\text{dis}} = N(\overline{\langle Q^2 \rangle_{\mathcal{C}_0}} - \overline{\langle Q \rangle_{\mathcal{C}_0}^2})$ . Clearly,  $\chi = \chi_{\text{dis}} + \chi_T$ . Numerical results, shown in Fig. 3(b), indicate that for the largest system the disorder fluctuations increase much more rapidly than thermal ones,

$$\chi_{\text{dis}} \propto \chi_T^2, \quad (1)$$

implying that the disorder should eventually completely dominate the behaviour of the total susceptibility,  $\chi \approx \chi_{\text{dis}} \gg \chi_T$ . Physically, Eq. (1) can be understood by assuming that fluctuations are completely dominated by the sample fluctuations of the field  $\epsilon_{\mathcal{C}_0}^*$ . In that case, standard results for ensemble-dependence of fluctuations [33–35] yield  $\chi_{\text{dis}} \approx N \text{Var}(\epsilon^*) \chi_T^2 / T^2$ , where  $\text{Var}(\epsilon^*)$  is the variance of  $\epsilon_{\mathcal{C}_0}^*$  among samples. The resulting scaling relation (1) is characteristic of the RFIM universality class. It is exact in mean-field analysis [12], and the deviations predicted from nonperturbative renormalization treatments in  $d = 3$  [36] are too small to be numerically observable [37]. Interestingly, the ratio  $\chi_{\text{dis}} / \chi_T^2$  provides a measure of the (effective) variance of the field, which is a dimensionless measure of the strength of the disorder in the effective RFIM description of the critical point [13]. It would be interesting to perform similar measurements for other models to perform a quantitative comparison of effective theories for different liquids [38].

The distribution  $P(Q)$  allows an estimation of the surface tension  $\Upsilon(T)$ , provided the first-order transition regime characterized by well-separated peaks can be accessed. Unfortunately, the computational effort required

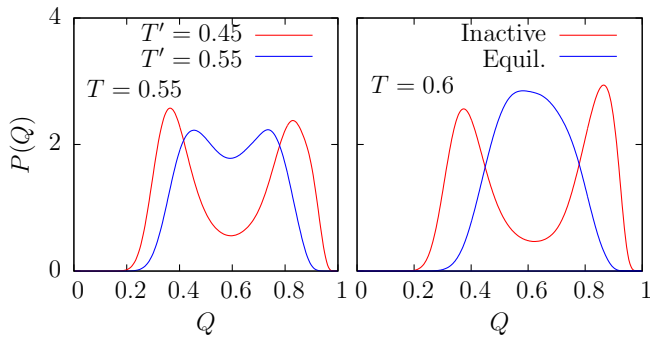


FIG. 4: (a) Comparison of distributions  $P(Q)$  and  $T = 0.55$ , for  $T' = T$  and  $T' = 0.45$ , at their corresponding fields  $\epsilon^*$ . (b) Comparison at  $T = 0.6$  between equilibrated  $\mathcal{C}_0$  at  $T' = 0.6$  and (biased) inactive  $\mathcal{C}_0$ . In both cases, the more stable states are associated with strongly bimodal  $P(Q)$ , indicating that coexistence between these low-energy states and the equilibrium fluid incurs a significant interfacial free energy cost.

to sample  $P(Q)$  for  $T \ll 0.55$  is prohibitive. To circumvent this difficulty, we exploit the flexibility offered by the independent sampling of configurations  $\mathcal{C}$  and  $\mathcal{C}_0$ . When  $T' \neq T$ , mean-field theory predicts that the three-parameter space  $(\epsilon, T, T')$  contains a line of RFIM critical points. The phase diagram in Fig. 1(c) corresponds to the  $T' = T$  plane in that space, but fixing for instance  $T' = 0.45$  should yield another critical point  $(\tilde{\epsilon}_c, \tilde{T}_c)$ . If  $\tilde{T}_c > T_c$ , then sampling temperatures below  $\tilde{T}_c$  should be easier. This is demonstrated in Fig. 4(a) where  $P(Q)$  for  $(T', T) = (0.45, 0.55)$  shows dramatically enhanced bimodality as compared to  $T' = T = 0.55$ . The natural inference is that the reduction in  $T'$  has resulted in an increase of the critical temperature, so that  $T = 0.55$  is now effectively deeper into the coexistence region. Thus, we interpret the free energy minimum in  $P(Q)$  as an interfacial cost, now corresponding to the spatial coexistence of equilibrium states at temperatures  $T'$  and  $T$ .

We show in Fig. 4(b) a similar comparison for  $T = 0.6$  where configurations  $\mathcal{C}_0$  at taken either from equilibrium at  $T' = 0.6$ , or sampled from the non-equilibrium  $s$ -ensemble at that same temperature with a biasing field towards atypically low dynamical activity [20, 21]. In terms of inherent structure energies, these inactive states represent glasses with very low fictive temperatures,  $T' \approx 0.4$  [21]. We observe again strong bimodality, in contrast to the corresponding equilibrium behaviour, which has nearly Gaussian fluctuations. The free-energy minimum in  $P(Q)$  is the interfacial cost between low- $Q$  states (typical of the equilibrium fluid at  $T = 0.6$ ), and high- $Q$  states (stable glassy states).

The results in Fig. 4(a,b) are significant because they directly evidence the existence of a free-energy cost for spatial coexistence between amorphous states. For  $(T' = 0.45, T = 0.55)$  we obtained data for  $N = 150$  and 256 and find that this cost increases with  $N$ . Additional sys-

tem sizes are needed to infer a numerical value for  $\Upsilon$ , via the scaling  $\Delta F \sim \Upsilon L^\theta$ . The exponent  $\theta$  is not known, but should obey  $\theta \leq d - 1$ , because interfaces can use quenched disorder to optimize their geometry and reduce their cost [31]. Physically the existence of an interfacial cost for the coexistence of stable glassy configurations with the equilibrium fluid, as in Fig. 3(b), suggests that nucleation and growth is the appropriate mechanism to interpret the kinetic stability and melting dynamics of ultrastable glasses [22, 23]. Systematic studies along the present lines should help understanding kinetic stability from first-principles.

We have presented the results of extensive free-energy calculations in supercooled liquids to assess the existence of thermodynamic singularities in constrained supercooled liquids, and to explore their consequences. Overall, our results are consistent with effective field theories predicting the existence of a random critical point, associated (below  $T_c$ ) with phase coexistence between metastable states. These results are also consistent with static correlations on length scales comparable with our largest system size [39, 40]. Whatever the status of the phase transition in the thermodynamic limit, we find that significant static fluctuations are present at a temperature  $T \leq 0.55$ , where dynamics is glassy. Note that if the critical point in this system is indeed at  $T_c \approx 0.55$ , a significant surface tension  $\Upsilon$  only exists when  $T \ll 0.55$ . Thus, the emergence of activated dynamics between metastable states might well fall out of the dynamic range currently accessible to simulations. Our approach generically allows the determination of  $\Upsilon$  in any material (including hard spheres), and extends to stable glassy states. This offers the potential for quantitative analysis of glass stability based on surface and bulk free energies. Overall, while our results do not speak directly to the mechanism of structural relaxation in glasses and supercooled liquids, they provide direct evidence that an interfacial free-energy barrier between metastable states is relevant both in the ‘melting’ of stable glasses and in glassy dynamics at equilibrium.

We thank G. Biroli, D. Coslovich and G. Tarjus for discussions. The research leading to these results has received funding from the European Research Council under the European Union’s Seventh Framework Programme (FP7/2007-2013) / ERC Grant agreement No 306845. RLJ was supported by the EPSRC through grant EP/I003797/1.

- 
- [1] L. Berthier and G. Biroli, *Rev. Mod. Phys.* **83**, 587 (2011).
  - [2] J.-P. Hansen and I.R. McDonald, *Theory of Simple Liquids*, 2nd ed. (Academic Press, London, 1986).
  - [3] L. Berthier and G. Tarjus, *Phys. Rev. Lett.* **103**, 170601 (2009).
  - [4] V. Lubchenko and P. G. Wolynes, *Annu. Rev. of Phys.*

- Chem. **58**, 235 (2007).
- [5] T.R. Kirkpatrick, D. Thirumalai and P.G. Wolynes, Phys. Rev. A **40**, 1045 (1989).
- [6] S. Franz and G. Parisi, Phys. Rev. Lett. **79**, 2486 (1997).
- [7] C. Cammarota, A. Cavagna, I. Giardina, G. Gradenigo, T. S. Grigera, G. Parisi and P. Verrocchio, Phys. Rev. Lett. **105**, 055703 (2010).
- [8] J. Yeo and M. A. Moore, Phys. Rev. E **86**, 052501 (2012).
- [9] L. Berthier, Phys. Rev. E **88**, 022313 (2013).
- [10] L. Berthier and D. Coslovich, Proc. Natl. Acad. Sci. USA **111**, 11668 (2014).
- [11] C. Cammarota and G. Biroli, J. Chem. Phys. **138**, 12A547 (2013).
- [12] S. Franz and G. Parisi, J. Stat. Mech. p. P11912 (2013).
- [13] G. Biroli, C. Cammarota, G. Tarjus and M. Tarzia, Phys. Rev. Lett. **112**, 175701 (2014).
- [14] J. Kurchan, G. Parisi and M. A. Virasoro, J. Phys. I **3**, 1819 (1999).
- [15] S. Franz and G. Parisi, Physica A **261**, 317 (1998).
- [16] M. Cardenas, S. Franz and G. Parisi, J. Chem. Phys. **110**, 1726 (1999).
- [17] J.-P. Bouchaud and G. Biroli, J. Chem. Phys. **121**, 7347 (2004).
- [18] C. Cammarota, A. Cavagna, G. Gradenigo, T. S. Grigera, and P. Verrocchio J. Stat. Mech. L12002 (2009).
- [19] C. Cammarota, A. Cavagna, G. Gradenigo, T. S. Grigera, and P. Verrocchio, J. Chem. Phys. **131**, 194901 (2009).
- [20] L. O. Hedges, R. L. Jack, J. P. Garrahan and D. Chandler, Science **323**, 1309 (2009).
- [21] R. L. Jack, L. O. Hedges, J. P. Garrahan, and D. Chandler, Phys. Rev. Lett. **107**, 275702 (2011).
- [22] A. Sepulveda, M. Tyllinski, A. Guiseppi-Elie, R. Richert, and M. D. Ediger, Phys. Rev. Lett. **113**, 045901 (2014).
- [23] G. M. Hocky, L. Berthier, and D. R. Reichman, J. Chem. Phys. **141**, 224503 (2014).
- [24] W. Kob and H. C. Andersen, Phys. Rev. E **51**, 4626 (1995).
- [25] R. Monasson, Phys. Rev. Lett. **75**, 2847 (1995).
- [26] M. Mézard, Physica A **265**, 352 (1999).
- [27] J. P. Garrahan, Phys. Rev. E **89**, 2014 (2014).
- [28] G. Parisi and B. Seoane, Phys. Rev. E **89**, 022309 (2014).
- [29] J.-M. Bomont, G. Pastore and J.-P. Hansen, EPL **105**, 36003 (2014).
- [30] C. Domb and M. S. Green, *Phase Transitions and Critical Phenomena. Vol. 2.* (Academic Press, London, 1972).
- [31] T. Nattermann, in *Spin Glasses and Random Fields*, Ed.: A. P. Young (World Scientific, Singapore, 1998).
- [32] D. S. Fisher, Phys. Rev. Lett. **56**, 416 (1986).
- [33] M. Schwartz and A. Soffer, Phys. Rev. Lett. **55**, 2499 (1985).
- [34] L. Berthier, G. Biroli, J.-P. Bouchaud, L. Cipelletti, D. El Masri, D. L'Hôte, F. Ladieu, and M. Pierno, Science **310**, 1797 (2005).
- [35] L. Berthier, G. Biroli, J.-P. Bouchaud, W. Kob, K. Miyazaki and D. R. Reichman, J. Chem. Phys. **126**, 184503 (2007); J. Chem. Phys. **126**, 184504 (2007).
- [36] G. Tarjus, I. Balog, and M. Tissier, EPL **103**, 61001 (2013).
- [37] N. G. Fytas and V. Martin-Mayor, Phys. Rev. Lett. **110**, 227201 (2013).
- [38] J. D. Stevenson, A. M. Walczak, R. W. Hall and P. G. Wolynes, J. Chem. Phys. **129**, 194505 (2008).
- [39] R. L. Jack and L. Berthier, Phys. Rev. E **85**, 021120 (2012).
- [40] C. J. Fullerton and R. L. Jack, Phys. Rev. Lett. **112**, 255701 (2014).